Solar Energy Materials & Solar Cells 147 (2016) 115–126

Contents lists available at ScienceDirect

Solar Energy Materials & Solar Cells

journal homepage: www.elsevier.com/locate/solmat

Review

Review of light-induced degradation in crystalline silicon solar cells

Jeanette Lindroos [a,b,*], Hele Savin [b]

[a] Department of Engineering and Physics, Karlstad University, Universitetsgatan 2, 65188 Karlstad, Sweden
[b] Department of Micro- and Nanosciences, Aalto University, Tietotie 3, 02150 Espoo, Finland

ARTICLE INFO

Article history:
Received 1 October 2015
Received in revised form
27 November 2015
Accepted 30 November 2015
Available online 23 December 2015

Keywords:
Boron
Copper
Degradation
Oxygen
Silicon
Solar cell

ABSTRACT

Although several advances have been made in the characterization and the mitigation of light-induced degradation (LID), industrial silicon solar cells still suffer from different types of light-induced efficiency losses. This review compiles four decades of LID results in both electronic- and solar-grade crystalline silicon. The review focuses on the properties and the defect models of boron-oxygen LID and copper-related LID. Current techniques for LID mitigation are presented in order to reduce cell degradation and separate copper-related LID from boron-oxygen LID. Finally, the review summarizes recent observations of severe LID in modern multicrystalline silicon solar cells.

© 2015 Elsevier B.V. All rights reserved.

Contents

* Corresponding author.
E-mail address: jeanette.lindroos@kau.se (J. Lindroos).

http://dx.doi.org/10.1016/j.solmat.2015.11.047
0927-0248/© 2015 Elsevier B.V. All rights reserved.

1. Introduction

Light-induced degradation (LID) refers to a loss in the silicon solar cell efficiency that is observed during excess carrier injection by above-bandgap illumination [1] or forward biasing [2]. LID is seen as a decrease in the solar cell short-circuit current and the open-circuit voltage [3], caused by increased minority-carrier recombination in the bulk of crystalline silicon [4]. Although LID has been studied extensively for the past four decades, the recombination-active defects responsible for degradation remain yet to be identified.

In the 1970s, LID was first observed in both electron- and proton-irradiated boron-doped Float Zone (FZ) silicon solar cells [3,5,6]. LID was measured also in 1 Ω-cm Czochralski (Cz) solar cells [6], with electron irradiation further decreasing the cell power, rendering both FZ-Si and Cz-Si unsatisfactory for space applications. Since unirradiated FZ-Si remained free of LID, the first LID results compiled by Curtin and Statler [7] were soon forgotten, and all efforts were focused on understanding LID in Cz-Si solar cells. Once the light-induced defect density was observed to increase with increasing boron and oxygen concentrations, degradation was linked to the formation of a boron-oxygen complex, and the effect became known as boron-oxygen LID (BO-LID) [4,8]. BO-LID is characterized by a fast initial decrease and a second slower decay [9–11] that are fully reversible at 200 °C [6]. The current B-O complex model has been questioned after the observation of similar LID in aluminum-doped Cz-Si, together with indium-doped Cz-Si and FZ-Si [12,13].

Minimizing either the boron or the oxygen concentration was presumed to guarantee LID-free silicon [14], until Henley et al. [15] measured LID in boron-doped FZ-Si with intentional copper contamination in 1998. After interstitial copper contamination was observed to induce degradation also in phosphorous- [16] and gallium-doped silicon [17], the effect became known as copper-related LID (Cu-LID). Copper was initially dismissed as a source of LID in solar cells, as most bulk copper contamination was presumed to have gettered during emitter formation [18–21] and/or back contact firing [22]. However, copper contamination was later observed to cause increased LID in multicrystalline (mc) Aluminum Back-Surface Field (Al-BSF) cells from the top of the ingot [23], where copper is known to collect during crystallization [24].

Interestingly, several solar cell manufacturers have recently observed strong LID in Passivated Emitter Rear Cells (PERC) and Al-BSF silicon solar cells, which cannot be explained by BO-LID theory or light-sensitive iron-boron pairs (FeB) [25–30]. In order to improve LID identification in modern solar cells, this review compiles and compares properties of the two recognized degradation effects: BO-LID and Cu-LID. Section 2 reports on boron-oxygen LID in monocrystalline silicon and solar cells. Section 3 compiles properties of copper in silicon and reviews results on copper-related LID. The known properties of Cu-LID are compared to BO-LID in Section 4. Finally, Section 5 expands into LID in low-cost quasi-mono and multicrystalline silicon solar cells, with conclusions presented in Section 6. The manuscript is based on the literature overview in J. Lindroos' doctoral dissertation [31].

2. Boron-oxygen degradation

Fig. 1 shows typical BO-LID measured in clean B-doped Cz-Si [32] with an oxygen concentration above 1 ppm [8,14]. The degradation is first observed as a fast initial exponential decrease (FRC) of the minority carrier lifetime or solar cell efficiency, followed by a second slower asymptotic decay (SRC) [9–11], which dominates the degradation. The effect is called boron-oxygen degradation (BO-LID), even though boron and oxygen are yet to be confirmed responsible for the recombination-active defect formation.

Despite the name of light-induced degradation, photons are not directly involved in the formation of BO-LID. As long as the photon energy exceeds the silicon bandgap, the photon wavelength and the penetration depth are irrelevant [1], since LID is in fact caused by the injection of excess minority carriers [33]. Therefore, full BO-LID is formed also during forward biasing of the cell in the dark [33]. Although BO-LID is observed at excess-carrier concentrations as low as 1.7×10^9 cm^{-3} [34], excess carriers cannot alone account for the defect density formed during degradation [35]. Instead, Bothe et al. [2] confirmed that BO-LID formation is determined by the *total* minority carrier concentration, based on BO-LID observation in the dark at zero bias at temperatures above 300 K. Therefore, controlling the temperature and the carrier injection conditions are paramount in determining the degradation rate and the normalized defect density of the fast (FRC) and the slow (SRC) recombination centers.

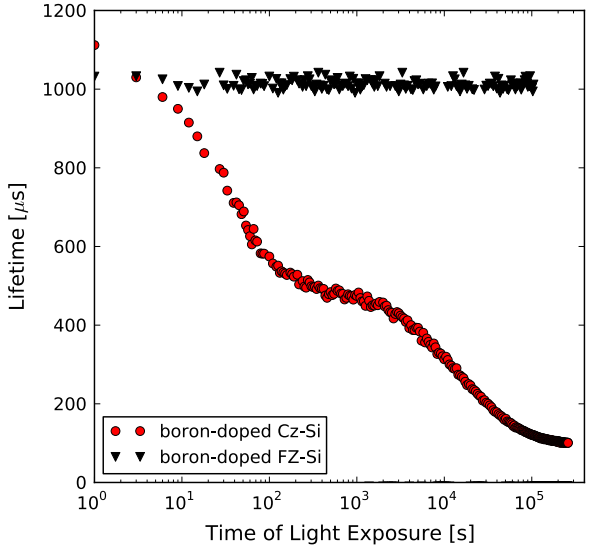

Fig. 1. Effective minority-carrier recombination lifetime as a function of illumination time in clean low-resistivity B-doped Cz-Si and FZ-Si [32]. (Reprinted with permission from Nærland, Characterization of light induced degradation in crystalline silicon, Norwegian University of Science and Technology, Trondheim, Norway, Vol. 2013:303 (2013). Copyright 2013, Nærland.)

2.1. Degradation kinetics

The degradation rate and the normalized defect density is most accurately obtained by measuring the decrease of the solar cell open-circuit voltage V_{OC} [2,36,37] or the decay of effective minority carrier recombination lifetime as a function of time. The effective recombination lifetime τ_{eff} in Fig. 1 is determined by the surface (τ_s), the Shockley-Read-Hall (τ_{SRH}), the radiative (τ_{rad}), and the Auger (τ_{Aug}) recombination lifetimes. Radiative recombination is negligible in silicon, and Auger recombination dominates only at high injection levels [38]. At low injection levels, the Shockley-Read-Hall recombination lifetime in p-Si is approximated by the minority carrier recombination lifetime τ_n. Thus, the recombination rate R becomes [38]

$$R=\frac{\Delta n}{\tau_{\text{eff}}}=\Delta n\left[\frac{1}{\tau_s}+\left(\frac{1}{\tau_{\text{SRH}}}+\frac{1}{\tau_{\text{rad}}}+\frac{1}{\tau_{\text{Aug}}}\right)\right]\approx\Delta n\left[\frac{1}{\tau_s}+\frac{1}{\tau_n}\right]\approx\Delta n\left[\frac{1}{\tau_s}+\sigma_n\nu_n N_t\right], \tag{1}$$

where Δn is the excess electron concentration, σ_n is the electron-capture cross-section of the recombination-active defect, ν_n is the mean thermal electron velocity, and N_t is the defect density. Consequently, the density of the light-induced defects N_t at illumination time t can be determined from the difference between the recombination rate $R(t)$ and the initial recombination rate $R(0)$ in Eq. (1) according to

$$R(t)-R(0)=\Delta n\left[\frac{1}{\tau_{\text{eff}}(t)}-\frac{1}{\tau_{\text{eff}}(0)}\right]=\Delta n\left[\left(\frac{1}{\tau_s(t)}+\frac{1}{\tau_n(t)}\right)-\frac{1}{\tau_s(0)}\right]=$$
$$=\frac{\Delta n}{\tau_n(t)}=\Delta n\sigma_n\nu_n N_t(t), \tag{2}$$

when the surface recombination lifetime remains constant during illumination ($\tau_s(t)=\tau_s(0)$), and all other recombination-active bulk defects are insensitive to light. Since σ_n is unknown, the *normalized* light-induced defect density $N_t^*(t)$ is defined as [8]

$$N_t^*(t)=\sigma_n\nu_n N_t(t)=\frac{1}{\tau_{\text{eff}}(t)}-\frac{1}{\tau_{\text{eff}}(0)}, \tag{3}$$

when the effective lifetimes are measured at the same low injection level. In most LID studies, effective lifetimes are reported at low injection levels near $\eta=\Delta n/p_0=0.1$ [10,39]. After long-term illumination, $N_t^*(t)$ approaches the saturated normalized defect density $N_{t,\text{sat}}^*$ of

$$N_{t,\text{sat}}^*=\frac{1}{\tau(\infty)}-\frac{1}{\tau(0)}. \tag{4}$$

BO-LID is thought to stem from a recombination-free latent defect that forms already during crystallization or wafer processing [40]. At any illumination time, the normalized latent defect density $N_t'(t)$ (of still recombination-free defects) can be obtained from the difference between the saturated normalized defect density $N_{t,\text{sat}}^*$ and the light-induced defect density $N_t^*(t)$ as

$$N_t'(t)=N_{t,\text{sat}}^*-N_t^*(t)=\frac{1}{\tau(\infty)}-\frac{1}{\tau(t)}. \tag{5}$$

The degradation rate R_{def} is then obtained by solving the differential equation of

$$-\frac{dN_t'(t)}{dt}=R_{\text{def}}N_t'(t),\quad \text{for}\quad \begin{matrix}N_t^*(0)=0; & N_t'(0)=N_{t,\text{sat}}^*\\ N_t^*(\infty)=N_{t,\text{sat}}^*; & N_t'(\infty)=0\end{matrix}. \tag{6}$$

The solution of Eq. (6) gives the normalized latent defect density $N_t'(t)$ of

$$N_t'(t)=N_{t,\text{sat}}^*\exp(-R_{\text{def}}t). \tag{7}$$

Through Eqs. (5) and (7), the degradation rate R_{def} and the degradation time constant τ_{def} can then be obtained by plotting the normalized light-induced defect density $N_t^*(t)$ as a function of time and fitting with [8]

$$N_t^*(t)=N_{t,\text{sat}}^*[1-\exp(-R_{\text{def}}t)]=\left(\frac{1}{\tau(\infty)}-\frac{1}{\tau(0)}\right)\left[1-\exp\left(-\frac{t}{\tau_{\text{def}}}\right)\right]. \tag{8}$$

2.2. Degradation rate

The FRC degradation rate R_{FRC} is obtained by applying Eq. (8) to the first exponential decay, while the SRC degradation rate R_{SRC} constant is determined by a separate fitting of the second asymptotic lifetime decrease. The slow degradation R_{SRC} shows no dependence on the illumination wavelength, when comparing blue (350–550 nm) and red light (> 800 nm) [1]. Although the illumination intensity was previously thought not to affect R_{SRC} above 1 mWcm^{-2} [1,10], Hamer et al. [41] recently measured a R_{SRC} increase as a function of increasing intensity from 44 to 3550 mWcm^{-2}.

R_{SRC} was first thought to increase with $[B_s]^2$ [37], until Macdonald et al. [42] observed a degradation rate proportionality to the equilibrium hole concentration p_0^2, in both boron-doped Si and phosphorus-compensated p-Si. However, as the total minority carrier concentration is known to determine the onset of BO-LID [2], and R_{SRC} increases with increasing intensity [41], Hamer et al. [41] have speculated that R_{SRC} could be proportional to the total hole concentration (p^2 or p_0p), instead of p_0^2.

2.3. Activation energy

The activation energy E_{def} of BO-LID is obtained by degrading Cz-Si at different temperatures and performing an Arrhenius fit to the degradation rate R_{def} with

$$R_{\text{def}}(T)=\kappa_0\exp(-E_{\text{def}}/k_BT). \tag{9}$$

In clean Cz-Si, fast degradation (FRC) is associated with the activation energy of 0.23 ± 0.02 eV and slow degradation (SRC) with 0.475 ± 0.035 eV [36]. The activation energies show no dependency on the wafer boron or oxygen concentration, but the pre-exponential κ_0 is found to increase with increasing boron doping [36].

2.4. Energy level

Injection- and temperature-dependent lifetime spectroscopy (IDLS and TDLS) have been used to estimate a deep SRC energy level at $E_C-0.41$ eV [43] with the carrier-capture cross-section ratio of $\sigma_n/\sigma_p=10\pm1$ [43,44]. This level corresponds to recent Deep Level Transient Spectroscopy (DLTS) results, which indicate a minority carrier trap at $E_C-0.41$ eV with the capture cross-section of 10^{17} cm^2 and a light-induced defect density of at least 2.5×10^{13} cm^{-3} [45]. DLTS measurements also reveal a majority carrier trap at $E_V+0.37$ eV with $\sigma_p\sim10^{18}$ cm^2 and a defect density of 2×10^{12} cm^{-3} [45]. Recent IDLS results support the notion of a second SRC defect level, but its position at $E_V+0.26$ eV is yet to be confirmed by TDLS [46].

IDLS combined with TDLS have indicated that the FRC level lies in the range of $E_V+(0.27\ldots0.77)$ eV with $\sigma_n/\sigma_p=100\pm10$ [36]. Voronkov et al. [47] estimate a FRC donor level (+1/0) with $\sigma_n/\sigma_p=65\pm1$ in p-Si and a FRC acceptor level (0/−1) at $E_V+(0.28\pm0.03)$ eV with $\sigma_n/\sigma_p=86\pm1$ in compensated n-Si. The latent recombination center present before FRC formation is determined to possess an energy level of $E_V+(0.635\pm0.020)$ eV [35,36]. The initiation of FRC formation is attributed to a latent defect charge change (from +1 to 0), due to an electron quasi-Fermi level shift across the latent defect energy level [36].

2.5. Recovery

Full dissociation of both FRC and SRC defects is observed after annealing at 200 °C in the dark [6], prompting both defects to be classified as metastable [10]. The SRC defect is shown to recover with the activation energy of 1.36 ± 0.06 eV [48], while FRC recovery is observed as a two-step process with the activation energies of 0.32 ± 0.01 eV and 1.36 ± 0.08 eV [36]. The dark recovery rate is found to be inversely proportional to the equilibrium hole concentration p_0 [48]. However, subsequent illumination reforms the same normalized light-induced defect density with the same degradation rate, as before the 200 °C recovery anneal [6].

2.6. Responsible defect

Although the BO-LID defects are yet to be identified, both current defect models agree on the involvement of the dopant acceptor. The first model is based on the activation of latent B_iB_sO [39], while the second proposes an acceptor and silicon self-interstitial pair [12,13].

2.6.1. Boron-oxygen complex

Several clues about the composition of the BO-LID defects are obtained from the saturated normalized defect density $N^*_{t,sat}$, which is defined in Eq. (4). Some studies in B-doped Si [10,36] and gallium co-doped p-Si [49,50] first found $N^*_{t,sat}$ to be proportional to $[B_s]$, while others later observed a net doping $p_0 = N_A - N_D$ dependency in p-Si compensated with phosphorus [42,51,52] or thermal donors [53]. Although some report no relation between the normalized defect density and the boron or the oxygen concentration [32], results indicating a $N^*_{t,sat}$ dependency on both p_0 and $[O_i]^2$ attribute the degradation to the formation of a boron-oxygen complex [10,36].

As experimental data accumulated, the proposed boron-oxygen complex changed from B_iO_i [4] to B_sO_{2i} [10], and to a combination of B_sO_{2i} (FRC) and B_iO_{2i} (SRC) [40,47]. After eliminating the involvement of oxygen dimers (O_{2i}) [54], Voronkov and Falster [39] proposed that FRC starts from latent B_sO_2 complexes and SRC from latent X_iB_sO, where X is a fast-diffusing interstitial impurity with $+1$ charge, which exists mostly in a precipitated state such as boron. In this model, B_iB_sO is presumed to form at low temperatures through B_iO dissociation and consequent B_i reaction with B_sO. Thus, the frozen-in concentration of latent B_iB_sO is thought to be proportional to both p_0 and $[O_i]^2$, even though the complex only contains one oxygen atom. B_iB_sO is thought to reconfigure into SRC during illumination, changing charge state from 0 to -1.

2.6.2. Acceptor and silicon self-interstitial pair

Recently, fast and slow LID was observed in aluminum-doped Cz-Si, in addition to indium-doped Cz-Si and FZ-Si, with full recovery at 200 °C [12,13]. Although the low initial lifetime in Al-doped Cz-Si is attributed to the formation of an aluminum-oxygen complex [55–57], the metastable degradation cannot be explained by B-O complex formation. Instead, Möller and Lauer [12,13] propose that BO-LID is caused by a charge-state change (from $+1$ to 0 to -1) of a near-substitutional acceptor and silicon self-interstitial pair ($A_{Si}Si_i$). The involvement of Si self-interstitials is based on initial LID observations in irradiated boron-doped FZ-Si [3,5,6]. However, those studies are inconclusive about the effect of 200 °C annealing, since Graff and Pieper [5] observed full recovery, while Fischer and Pschunder [6] measured further degradation in irradiated FZ-Si. In addition, Caballero et al. [58] found no correlation between the injection of Si self-interstitials and BO-LID in Cz-Si.

2.7. Mitigating degradation

2.7.1. Minimizing boron and oxygen

Boron-oxygen LID is traditionally mitigated by minimizing the concentration of boron or oxygen in the silicon bulk [8]. Reducing the oxygen concentration below 1 ppm is effective, as no LID has been measured in clean boron-doped FZ-Si (Fig. 1) or 5.2 Ω-cm magnetic Czochralski (MCz) Si with 0.99 ppm of oxygen [8,14]. However, low-oxygen MCz-Si and FZ-Si ingot growth are known to be more expensive than conventional Cz-Si.

Replacing the boron doping with gallium proves also effective, as no BO-LID has been measured in gallium-doped Cz-Si, regardless of oxygen concentration [4,14] or electron irradiation dose [59]. However, the low segregation coefficient of gallium makes the growth of uniform-resistivity ingots challenging [60]. BO-LID can additionally be mitigated by replacing the solar cell bulk with n-Si, since no degradation has been measured in clean phosphorus-doped Cz-Si [4] or phosphorus-doped FZ-Si with an increased oxygen level of 8.4 ppm [61].

2.7.2. Regeneration

In Cz-Si with BO-LID, Herguth et al. [62] have deactivated the metastable defects completely by the means of simultaneous illumination and annealing at 65–210 °C [62–64], known as regeneration. During regeneration, the metastable defect is formed during the first few minutes of illumination at an elevated temperature but then dissociated with the activation energy of 0.61 – 0.98 eV [62–65]. The regeneration rate is inversely proportional to the boron concentration [66] and directly proportional to the oxygen concentration [67]. The regeneration time is shown to vary from 10 s [65] to several hours depending on the illumination intensity, illumination temperature, and the surface passivation [63]. The passivation influence is thought to stem from the hydrogen concentration in the passivation layer [68], as the regeneration rate is observed to increase with increasing hydrogen content [65,69]. Hydrogen is assumed to form B-H pairs during regeneration [65], preventing BO-LID formation during subsequent illumination.

After optimized regeneration, further illumination causes no severe defect formation. However, annealing at 200 °C for 1 h is sufficient to completely destabilize the regenerated lifetime [70], resulting again in full BO-LID defect formation during subsequent illumination. Although full destabilization is observed already at 170 °C [65,71], the high destabilization activation energy of 1.25 $\pm$ 0.05 eV [65] only starts hindering regeneration (at 0.27 Wcm^{-2}), when the illumination temperature exceeds 230 °C [65]. Therefore, high-speed regeneration can be achieved at high hydrogen concentration and illumination intensity at $T < 230$ °C [72]. In practice, the high hydrogen concentration is achieved by PECVD deposition of SiN_x that is fired at high temperature, followed by fast quenching [73].

3. Copper-related degradation

In 1998, Henley et al. [15] and Tarasov et al. [74] observed light-induced degradation of the minority carrier diffusion length in $9-20$ Ω-cm p-type Cz-Si contaminated with copper concentrations lower than the doping level. Henley's samples were oxidized to prevent copper out-diffusion [75], and copper-related LID (Cu-LID) was separated from iron-related recombination by cyclic [74] and long-term [15] illumination. Later, Cu-LID was observed also in B-doped FZ-Si [16,76], >5 k Ω-cm P-doped FZ-Si [16], B-doped mc-Si [77], and Ga-doped Cz-Si [17], confirming that Cu-LID can occur in silicon regardless of acceptor, oxygen, or Si self-interstitial concentrations.

Copper is deemed to activate Cu-LID formation, since intentional copper contamination results in LID in Ga-doped Cz-Si [4,14], which is free of BO-LID even after electron irradiation [59]. In addition, Total Reflection X-Ray Fluorescence (TXRF) measurements confirm that Cu-LID is inhibited by the removal of copper from the wafer bulk [78], which is discussed in detail in Section 3.8. Interstitial copper (Cu_i) is specifically thought to be a prerequisite for Cu-LID formation, since Transient Ion Drift (TID) measurements show a Cu_i loss during illumination [79], the Cu-LID defect density is proportional to the initial [Cu_i] [80], and Cu_i removal prevents Cu-LID [78,81–86].

3.1. Interstitial copper

Copper is a 3*d* transition metal that diffuses interstitially in silicon as a positively charged ion (Cu_i^+) [87,88]. In intrinsic Si and *n*-type Si, TID measurements have revealed the diffusion activation energy of 0.18 ± 0.01 eV [89], which matches the most recent first-principles calculations [90] obtained with the Nudged Elastic Band (NEB) [91–94] method.

In *p*-type Si, interstitial copper pairs with negatively charged acceptor atoms, forming CuB, CuGa, CuAl, and CuIn. However, such pairs are unstable at RT, resulting in merely a decreased effective copper diffusivity. Diffusion is slower in Ga-doped Si than in B-Si, due to the higher dissociation energy of CuGa (0.71 ± 0.02 eV) compared to CuB (0.61 ± 0.02 eV) [89,95]. The dissociation energy of CuAl and CuIn have been measured as 0.70 eV [95]. In B-doped silicon, the effective diffusivity $D_{Cu,eff}$ is determined as [89]

$$D_{Cu,eff}(T) = \frac{(3 \times 10^{-4})\exp(-2090/T)}{1+(2.584 \times 10^{-20})\exp(4990/T)(N_A/T)}\ \mathrm{cm^2 s^{-1}}, \quad (10)$$

when the boron concentration $N_A < 10^{17}$ cm^{-3}. The effective diffusivity has been obtained in the temperature range of $-33 < T < 107$ °C. The solubility of interstitial copper has been measured as [88]

$$S_{Cu}(T) = 5 \times 10^{22}\exp\left(2.4 - \frac{1.49\ \mathrm{eV}}{k_B T}\right)\ \mathrm{cm^{-3}}, \quad (11)$$

when $500 < T < 800$ °C.

Cu_i^+ acts as a donor in silicon and is associated with the energy level of $E_C - 0.15$ eV (shown in Fig. 4) that has only been detected in *n*-Si [96]. After processing at elevated temperatures and air cooling, copper stays as interstitials in the bulk of low-defect B-doped Si, if the surface is oxide passivated (≥ 3 nm) [75], and [Cu] $\leq$ ([B]$+10^{16}$) cm^{-3} [97]. A bare surface or a thinner oxide will result in copper out-diffusion to the surface according to Eq. (10)

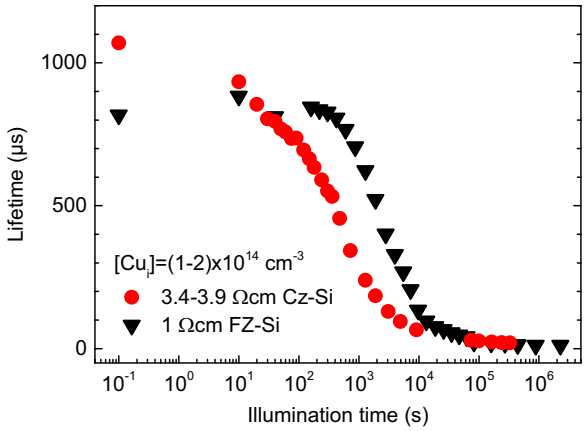

Fig. 2. Effective minority-carrier recombination lifetime as a function of illumination time in oxidized and copper-contaminated 3.4–3.9 Ω-cm Cz-Si and 1 Ω-cm FZ-Si measured with Quasi Steady State Photoconductance (QSSPC) at 0.15 Wcm^{-2}.

and consequent precipitation, which is known as haze formation [98–100]. A higher copper concentration or a high bulk defect density will cause partial copper precipitation in the bulk [98,99,101]. Interstitial bulk copper is not recombination active, and a lifetime increase has even been observed in B-doped Cz-Si at [Cu_i^+] $< 10^{14}$ cm^{-2} [102–106]. Therefore, interstitial bulk contamination goes unnoticed before illumination.

3.2. Degradation rate

Fig. 2 shows Cu-LID in intentionally contaminated low-resistivity B-doped Cz-Si and FZ-Si, where the bulk copper is interstitial before illumination. In B-doped FZ-Si, Cu-LID is observed as a single exponential degradation that can be fitted with the same decay function as BO-LID in Eq. (8) [15,16,76]. Single exponential decay is also observed in P-doped FZ-Si [16], Ga-doped Cz-Si [17], and B-doped mc-Si [77]. However, copper-contaminated B-doped Cz-Si (that already suffers from BO-LID) exhibits fast initial degradation, followed by a second slower decay, and a final very slow lifetime decrease [81].

The degradation rate of Cu-LID is found to increase with increasing temperature [81], illumination intensity [76,82], interstitial copper concentration [16,80], and bulk micro-defect (BMD) density [80,83,107]. In both B-doped and Ga-doped Cz-Si [17,81], the degradation rate is observed to increase with decreasing doping concentration, which could be explained by a decreasing concentration of copper-acceptor pairs that need to dissociate before Cu-LID formation.

3.3. Activation energy

In B-doped Cz-Si, the activation energy of the slow Cu-LID has been measured as 0.323 ± 0.090 eV in 3.4–3.9 Ω-cm and 0.146 ± 0.025 eV in 18–24 Ω-cm wafers, respectively [81]. Therefore, the Cu-LID activation energy appears to increase with increasing boron concentration, which could be caused by an increasing CuB concentration and decreasing copper diffusivity. In high-resistivity Si, the activation energy is surprisingly low and close to the intrinsic diffusion energy of 0.18 ± 0.01 eV [89]. Therefore, the measured Cu-LID activation energies might reflect the diffusivity of copper, instead of the formation energy of Cu-LID. This interpretation makes copper diffusion the limiting reaction in the formation of copper-related LID. However, diffusion-limited Cu-LID would result in the formation of a low density of copper-related defects, which is less likely to cause such a large lifetime decrease, as shown in Fig. 2.

3.4. Defect density

In Cu-contaminated Cz-Si, the saturated normalized defect density $N_t^*(\infty)$ is found to increase with increasing bulk micro-defect (BMD) density [83,107] and be proportional to the interstitial copper concentration [80]. Therefore, $N_t^*(\infty)$ can be used to estimate the initial interstitial copper concentration C_{Cu} in defect-free silicon by [80]

$$C_{Cu} = \sqrt{\frac{N_t^*(\infty)}{(4.0 \pm 0.5) \times 10^{-24}}}\ (\mathrm{cm^{-3}}), \quad (12)$$

and in silicon with high BMD density (10^{10} cm^{-3}) by [80]

$$C_{Cu} = \frac{N_t^*(\infty)}{(3.0 \pm 0.2) \times 10^{-8}}\ (\mathrm{cm^{-3}}), \quad (13)$$

when $N_t^*(\infty)$ is obtained by Microwave Photoconductance Decay (μ-PCD) lifetime measurements. The copper detection limit has been determined as some 5×10^{12} cm^{-3} in defect-free Si and

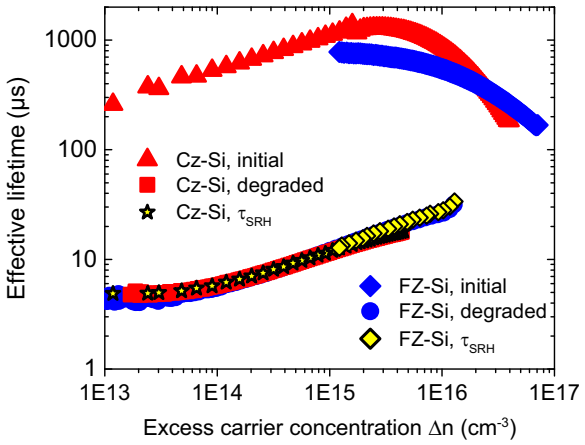

Fig. 3. Effective lifetime as a function of excess carrier density in copper-contaminated 3.4–3.9 Ω-cm Cz-Si and 1 Ω-cm FZ-Si measured with QSSPC before and after 0.15 Wcm^{-2} illumination. $\tau_{SRH}=1/N^{*}_{t,sat}$ refers to the SRH recombination lifetime caused by light-induced defects in Eq. (4).

below 10^{10} cm^{-3} in high-BMD density material such as mc-Si [80]. A higher BMD density is proposed to render Cz-Si more sensitive to lower copper concentrations compared to FZ-Si [16]. In contrast to the degradation rate, the normalized defect density is observed to increase with increasing boron concentration [81].

3.5. Recovery

In Cz-Si with Cu-LID, partial lifetime recovery is observed during 2 min of annealing at 200 °C [108], if the initial $[Cu_i] < 10^{14}$ cm^{-3}. Higher copper concentrations have resulted in no lifetime improvement at 200 °C [78,81,84]. Partial Cu-LID recovery is also measured in FZ-Si (at $[Cu_i] < 10^{14}$ cm^{-3}) [108], indicating that the lifetime increase is caused by the dissociation of Cu-LID defects. Although partial recovery is observed at 200 °C, full defect dissociation has only been measured after 1 min of rapid thermal annealing (RTA) at 900 °C [79]. Therefore, the dissociation experiments do not reveal the defect responsible for Cu-LID.

3.6. Responsible defect

Although illumination is shown to decrease the interstitial copper concentration [79], the resulting recombination-active defect remains unknown. Concerns about Cu-LID being mere surface recombination were raised by Boehringer et al. [109], after the observation of a light-induced increase in the Si/SiO_2 interface defect density D_{it}. However, Cu-LID was determined to predominantly cause bulk recombination, as no lifetime recovery occurred after surface removal [78], illumination above 0.5 Wcm^{-2} trapped copper in the bulk [79], and a D_{it} increase was also detected in clean reference wafers [81]. In addition, Fig. 3 shows the initial and the degraded effective lifetimes in Cu-contaminated Cz-Si and FZ-Si, together with the SRH bulk recombination lifetime, extracted through Eq. (4). As the SRH lifetime caused by recombination at Cu-LID defects coincides with the effective degraded lifetime, the degraded lifetime is clearly dominated by SRH bulk recombination.

During illumination, copper appears to act as either a catalyst for Cu-LID defect formation or an active part of the defect itself. The Cu-LID defect is likely to contain copper, since copper forms several recombination-active energy levels in the silicon bandgap, which are summarized in Fig. 4. Light-induced bulk recombination has been suggested to stem from copper precipitation [82] or the

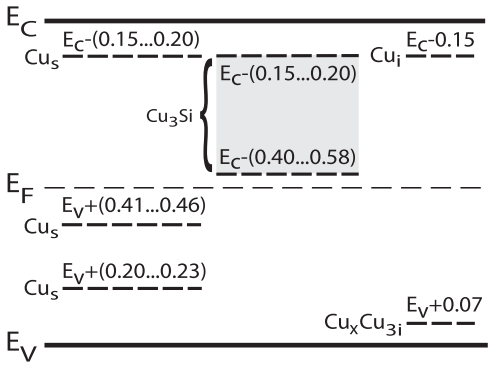

Fig. 4. Silicon bandgap with the three recombination-active energy levels of substitutional copper (Cu_s) [123–127,129–132] and the recombination-active energy band of copper precipitates (Cu_3Si) [101,142,143], together with the recombination-free levels of interstitial copper (Cu_i) [96] and the copper complex (Cu_xCu_{3i}) [110].

release of substitutional copper (Cu_s) through pure copper complex dissociation [15,76].

3.6.1. Substitutional copper

During illumination, Tarasov et al. [74] observed a decrease in the DLTS peak ($E_V+0.07$ eV [110]) of the recombination-free pure copper complex and consequent formation of new peaks deeper in the silicon bandgap [74]. The pure copper complex was long presumed to be a Cu_sCu_i pair [111,112], which led Henley et al. [15] and Ramappa [76] to suggest that illumination dissociates copper complexes, increasing the concentration of recombination-active Cu_s. The pure copper complex has since been determined to contain four copper atoms [113,114], out of which three are identified as Cu_i [115,116]. However, first principles calculations suggest that the fourth atom could still be substitutional copper [117–119].

Interstitial copper becomes Cu_s by occupying a vacancy, which releases 2.5 − 2.8 eV [87,120], or by kicking out a Si self-interstitial and one Si host atom, releasing 1.2 eV [121]. Interstitials also react with the oxygen-vacancy A center according to $Cu_i+\{O,V\}\rightarrow\{Cu_s,O_i\}$ at 175 − 250 °C, creating a defect level at $E_C-0.6$ eV [122]. This level corresponds to DLTS results that establish the $Cu_s^{0/-}$ level at $E_V+(0.41\ldots0.46)$ eV [123–127] with the estimated hole-capture cross-section of 1.5×10^{-14} cm^2 [128]. The two other DLTS levels presented in Fig. 4 are $E_V+(0.2\ldots0.23)$ eV ($Cu_s^{+/0}$) [123–126,129–132] and $E_C-(0.15\ldots0.2)$ eV ($Cu_s^{-/--}$) [123–125,130,132,133], with $\sigma_p=3\times10^{-14}$ cm^2 and $\sigma_n=1.9\times10^{-17}$ cm^2, respectively [128]. Cu_s is also known to form several complexes with hydrogen [119,121,134], while interstitial copper reacts only weakly with oxygen [121,135]. However, the concentration of Cu_s is usually less than 0.1% of the copper solubility [136].

The pure copper complex (Cu_xCu_{3i}) is identified by a sharp no-phonon Photoluminescence (PL) peak at 1014 meV [137], which is two orders of magnitude higher in FZ-Si compared to Cz-Si [138]. Copper complexes are shown to form with the activation energy of 0.57 ± 0.05 eV [139]. A decrease in the complex concentration is measured at 150 °C [140] with full complex dissociation at 250 °C [110,140]. After dissociation, DLTS measurements have revealed an energy level of $E_C-0.16$ eV at the Si surface [141]. Although this energy level corresponds to both Cu_i [96] and Cu_s [123–125,130,132,133], the defect level may not be related to copper complex dissociation, but reflect copper precipitation at the bare Si surface [141].

3.6.2. Copper precipitates

Interstitial copper precipitates as η''-Cu_3Si in crystalline silicon [144–147]. Copper precipitates cause severe minority-carrier recombination, since they form a deep defect band between $E_C-(0.15\ldots0.2)$ eV and $E_C-(0.4\ldots0.58)$ eV [101,142,143], as shown in

Fig. 4. The electron capture cross-section of Cu_3Si has been estimated as 3×10^{-16} cm^2 [148].

The precipitation of copper cannot simply be explained by impurity supersaturation and consequent precipitate formation at low nucleation barriers. In fact, interstitial copper has been shown to precipitate in the bulk only when the Fermi level exceeds $E_C - 0.2$ eV [97], which is the neutrality level of Cu_3Si. Below this energy level, Cu_3Si is positively charged and repels positively charged interstitial copper, preventing precipitation [101]. However, Cu_3Si becomes neutral or negative at $E_C - 0.2$ eV, enabling precipitate formation and growth. As the Fermi level depends on the doping concentration, the Cu_i donor concentration, and the temperature, these parameters determine the precipitate size and distribution together with the bulk defect density, the surface potential, and the thermal history.

In *n*-Si, the Fermi level exceeds $E_C - 0.2$ eV at $[P] = 1.7 \times 10^{16}$ cm^{-3}, resulting in precipitation at 300 K. Therefore, copper precipitates are common in the *n*-Si bulk, regardless of the copper concentration or the thermal history [103,105,106]. In defect-free B-doped Si, Cu_3Si reaches the neutrality level only when $[Cu] > ([B] + 10^{16})$ cm^{-3} [97]. Fast quenching of $[Cu] > 10^{17}$ cm^{-3} has revealed platelet-like precipitates (30 – 500 nm) mostly in the {111} plane, which are homogeneously distributed in the bulk up to densities of 10^{13} cm^{-3} [98,99,101]. Internal ripening of small homogeneous platelets into spherical precipitates is observed at 260–400 °C [98,149].

Slower cooling leads to less supersaturation and a longer time for Cu_i to diffuse towards the surface, resulting in a lower density of larger precipitate colonies heterogeneously distributed near the surface, known as haze [98–100]. The large lattice mismatch of 150% between Cu_3Si and Si causes stacking fault formation during precipitation [148]. As stacking faults provide a low nucleation barrier for copper precipitates, large copper colonies (0.5–80 μm) [147] consist of copper platelets surrounded by stacking faults that are decorated with small spherical precipitates [98,99]. In high defect-density Si, heterogeneous copper precipitation also occurs at stacking faults, dislocations, and higher sigma grain boundaries [150]. In addition, copper is shown to precipitate near oxygen precipitates [151].

The Fermi level can also be affected by illumination, as high-intensity light is known to generate electron and hole quasi-Fermi levels E_{Fn} and E_{Fp}, respectively [152]. When E_{Fn} exceeds $E_C - 0.2$ eV, Belayachi et al. [79] have noticed a significant trapping of Cu_i^+ in the bulk, while Yli-Koski [83] and Väinölä et al. [82] have observed a clear increase in the copper-related degradation rate. Therefore, Cu-LID has been suggested to originate from copper precipitation [82]. Light-induced copper precipitation is proposed to mainly occur as a result of Cu_3Si becoming neutral or negative during illumination, but a charge change of interstitial copper cannot be ruled out.

Assuming that the degradation rate is proportional to the precipitation rate and the precipitate size is fixed, the light-induced precipitate radius r and density n can be obtained from the degradation time constant τ_{def} in Eq. (8) by [153]

$$\tau_{def} = \left(4\pi n r D_{Cu,eff}\right)^{-1}, \quad (14)$$

where $D_{Cu,eff}$ is the effective copper diffusivity in Eq. (10) at the illumination temperature.

The time and temperature required to dissolve a specific size of spherical copper precipitate can be estimated based on the diffusivity (Eq. (10)) and solubility (Eq. (11)) at the annealing temperature, the precipitate copper concentration, and the sample copper concentration far from the precipitate [154]. Even though this model predicts the dissolution of precipitates with a radius smaller than 11 nm after 30 s at 500 °C [154], 10 min annealing at 200 °C would result in no precipitate dissociation.

3.7. Thermally induced recombination

Boron-oxygen LID is known to form during excess carrier injection and recover at 200 °C, regardless of whether the carrier injection is achieved by photon absorption, forward biasing, or a temperature increase [2]. Ramappa [76] has suggested that the same applies to Cu-LID, meaning that thermally induced carrier injection would cause the same degradation reaction as Cu-LID. Therefore, this subsection summarizes the lifetime behavior observed in unilluminated copper-contaminated FZ-Si and Cz-Si at RT to 200 °C.

Storage in the dark at RT leads to a minority carrier lifetime decrease in contaminated B-doped Cz-Si with a 16-nm thermal oxide and positive corona charge. Six days of dark storage decreases the lifetime from 891 to 720 μs in 3.4 Ω-cm Cz-Si and from 6.2 to 3.9 ms in 27 Ω-cm Cz-Si with $[Cu_i] = (1–2) \times 10^{14}$ cm^{-3}, respectively. A lifetime decrease during storage at 25 and 50 °C was also observed by Arumughan et al. [155] in *p*-type Cz-Si, although the wafers had not been intentionally contaminated by copper. The only link to unintentional contamination may have been the observation of a much faster LID effect than the expected BO degradation.

After 30 min of dark annealing at 75 °C, Ramappa and Henley observed a diffusion length increase in intentionally contaminated Cz-Si [156] and a decrease in FZ-Si [76]. The diffusion length decrease in FZ-Si had an activation energy of 0.419 eV. Ramappa [76] suggested that this thermally-induced decrease is caused by the same reaction as Cu-LID, making 0.419 eV the activation energy of Cu-LID in 1–2 Ω-cm B-doped FZ-Si. The proposed reaction was the dissociation of copper pairs (now known as copper complexes [113,114]) and subsequent release of recombination-active Cu_s. However, as copper complex dissociation is only observed above 150 °C [110,140], complex dissociation cannot explain the diffusion length decrease at 75–150 °C. Therefore, either Cu-LID and thermal degradation are caused by the same reaction that is not copper complex dissociation, or they are caused by different defects, with a possibility of complex dissociation resulting in Cu-LID.

Ramappa and Henley [156] first associated the Cz-Si diffusion length increase at 75 °C with thermal copper precipitation [157]. However, copper precipitation is unlikely, as precipitation conditions were not met ($E_F < E_C - 0.2$ eV [97]) and precipitation of interstitial copper is expected to decrease the effective diffusion length. Ramappa and Henley [156] eventually observed a diffusion length decrease also in Cz-Si, after increasing the temperature to above 100 °C and the annealing time to 60 min.

Since BO-LID is known to recover fully at 200 °C [6], clean Cz-Si is typically annealed at 200 °C before the start of illumination. However, in Cu-contaminated B-doped Cz-Si, pre-illumination annealing at 200 °C results mostly in lifetime decay [78,81]. Lifetime degradation at 200 °C may result from Cu_s formation by Cu_i reaction with oxygen-vacancy centers, as discussed in Section 3.6.1. The temperature is also high enough to dissolve copper complexes [110,140], potentially releasing Cu_s. Lifetime improvement at 200 °C was only observed in the case of short 2 min annealing and low-resistivity Cz-Si [81]. Although the temporary lifetime increase could have been caused by the recovery of BO-LID formed during sample preparation, the increase might also be related to the Cz-Si lifetime improvement observed at 75 °C by Ramappa and Henley [156].

3.8. Mitigating copper

In order to minimize copper-related recombination, several methods have been developed to decrease the bulk and surface copper concentrations. Methods applicable to bulk devices such as solar cells include copper out-diffusion and segregation gettering. For surface-active devices, the wafer copper concentration can be reduced by internal gettering, which relies on copper collection to [158] and precipitation near oxygen precipitates in the bulk [159,160].

3.8.1. Out-diffusion

In bare defect-free *p*-type Si, interstitial copper does not stay in the bulk but diffuses to the wafer surface in order to reach equilibrium solubility [161]. After out-diffusion, copper precipitates at the wafer surface, forming haze [98–100]. The out-diffusion time depends on the wafer thickness [97] and the effective copper diffusivity $D_{Cu,eff}(T)$ in Eq. (10) [89]. Out-diffusion has been shown to accelerate during continuous deposition of negative surface charges [162] (such as corona charges CO_3^-) that attract Cu_i^+. In some cases [75,163], accelerated out-diffusion has also occurred during annealing at 100–400 °C [164]. Recently, similar copper out-diffusion has been observed in bare *n*-Si with lower phosphorus concentrations [165]. After out-diffusion, the copper haze can be removed by silicon etching, but obtaining a clean surface is challenging, as copper tends to replate during chemical processing [128].

Copper out-diffusion is slowed down by a 0.2 V surface potential barrier [166] and completely prevented by a $3-4$ nm positively-charged oxide [75]. A 5-nm thermal oxide is shown to prevent copper out-diffusion even during annealing at 400 °C [167]. However, even in oxidized silicon, Cu_i^+ can be forced to diffuse towards the Si/SiO_2 interface by the deposition of a negative surface charge [31,78]. By optimizing the negative surface charge according to the initial $[Cu_i]$ [31,81,85], the bulk concentration can be reduced to a level below the Cu-LID detection limit [78,81–86]. For example, a cumulative charge density of -4.6×10^{12} cm^{-2} is required to remove $[Cu_i^+]=1.6\times10^{14}$ cm^{-2} from low-resistivity B-doped Cz-Si [81]. The deposition of Al_2O_3 with a charge density of -6.2×10^{13} cm^{-2} also prevented interstitial copper of 5×10^{12} cm^{-3} from forming Cu-LID in mc-Si [77].

Nevertheless, optimized negative surface charging is not sufficient to permanently prevent Cu-LID, as the redeposition of positive corona charges (H_3O^+) is shown to diffuse copper back into the bulk, causing Cu-LID [31,86]. Currently, Cu-LID has only been permanently prevented by negative charging followed by silicon surface etching [78] or negative charging combined with illumination [31]. However, further experiments are needed to understand how the illumination of near-surface collected copper prevents copper back-diffusion.

3.8.2. Segregation gettering

Phosphorus, boron, and aluminum gettering are well-known segregation gettering methods, which rely on copper diffusion at elevated temperatures into a P-doped layer, heavily B-doped layer, or an Al-Si liquid, due to a higher copper solubility [168,169]. Submitting the wafer to phosphorus diffusion gettering (PDG) around 900 °C over 60 min has been confirmed as a very efficient method to remove copper from the silicon bulk [18–21,31]. However, such a long PDG step is not comparable to most industrial emitter formation processes. PDG gettering has been modeled by the distribution of Cu_i, Cu_s and CuP pairs [169], but the experimental segregation coefficient is yet to be determined, as several experimental studies have reported copper concentrations below the detection limit after PDG [18,19]. Aluminum gettering for 2 h at 800 °C has resulted in a segregation coefficient of at least $(1-2)\times10^3$, estimating a 90% copper concentration decrease in a 240-μm-thick wafer with a 1 μm aluminum layer [22].

Table 1
Properties of boron-oxygen LID and copper-related LID.

Boron-oxygen LID	Copper-related LID
Faster with increasing T [36]	Faster with increasing T [81]
Light-intensity dependent [41]	Light-intensity dependent [76,82]
Defect density $\propto p_0$ [42,52]	More defects with increasing $[B_s]$ [81]
FRC and SRC [9–11,32]	One exp. [15–17,77] / Three exp. decay [81]
No occurrence in FZ-Si or Ga-Si [4,14,59]	Detected in FZ-Si [16,76] & Ga-doped Cz-Si [17]
Degradation rate $\propto p_0^2$ [42]	Slower with higher $[B_s]/[Ga_s]$ [17,81]
Defect density $\propto [O_i]^2$ [9,10,36,42,52]	Defect density $\propto$ $[Cu_i]$ and [BMD] [80]
E_{def} independent of $[B_s]$ [36]	E_{def} dependent on $[B_s]$ [81][a]
Full recovery at 200 °C [6]	Partial [108] or no recovery at 200 °C [81,84]
Unaffected by negative charge [31,81]	Removed by negative charge [78,77,82,83,85,86]

[a] E_{def} might reflect effective copper diffusivity instead of Cu-LID.

4. Comparison of boron-oxygen and copper-related degradation

Even though low-resistivity B-doped Cz-Si is observed to be the most sensitive Si material to both Cu-LID and BO-LID [16], the two degradation effects have several distinguishing properties, which are listed in Table 1. The BO degradation rate increases with increasing equilibrium hole concentration [42], while Cu-LID slows down with increasing doping concentration [17,81]. The activation energy of the BO-LID SRC is measured as 0.475 ± 0.035 eV [36] regardless of the doping concentration, but the Cu-LID activation energy is observed to increase with increasing boron concentration [81]. During 200 °C annealing, BO-LID recovers to its initial lifetime level [6], while wafers with Cu-LID show no [81,84] or only partial [108] recovery, depending on the initial interstitial copper concentration. Although Cu-LID is prevented by optimized negative surface charging followed by illumination or surface etching [31,78], the method shows no impact on BO-LID formation. Hence, BO-LID and Cu-LID are concluded to be two different degradation reactions, forming separate recombination-active defects.

Although BO-LID and Cu-LID are two different degradation effects, they may occur simultaneously in solar-grade silicon. Distinguishing between the two degradation effects in a single solar cell is still challenging, as both BO-LID and Cu-LID cause exponential lifetime decrease and recovery annealing at 200 °C may affect surface passivation [29,170]. Cz-Si can accurately be diagnosed to suffer from BO-LID, if the cell shows double exponential decay, full recovery at 200 °C, and full regeneration (under optimized conditions). In other cases, Cu-LID dominance may be suspected, but must to be confirmed by analyzing the initial interstitial copper concentration or by applying copper removal techniques, presented in Section 3.8. Therefore, further properties of Cu-LID need to be identified, in order to better distinguish between BO-LID and Cu-LID in industrial silicon solar cells.

5. Quasi-mono and multicrystalline silicon

In addition to monocrystalline silicon, LID has been observed in different types of quasi-mono (QuMo) and multicrystalline silicon. Some B-doped mc-Si [171–174] show less metastable decay than

the BO-LID observed in similar-resistivity Cz-Si, which is regarded as a result of a lower oxygen [171,173] or a higher carbon [174] concentration. Carbon is also suggested to slow down double exponential degradation in B-doped QuMo-Si [175]. Less degradation is expected in QuMo-Si and mc-Si simply due to a lower initial minority carrier recombination lifetime [172–174] caused by higher levels of transition metals and higher densities of extended defects, such as dislocations and/or grain boundaries. In mc-Si, Macdonald et al. [173] observed a super-linear defect density dependence on $[O_i]$ at low oxygen concentrations, which changes into a near-quadratic dependence at high oxygen concentrations. As the measured degradation varied greatly between grains, interstitial oxygen was suggested not to be directly involved in LID formation in mc-Si [173].

Other B-doped mc-Si exhibit stronger degradation than predicted by BO-LID theory [25–30]. Intentional copper contamination results in increased LID in mc-Si wafers [77] and Al-BSF cells [23] from the top of the ingot, where copper is known to collect during crystallization [24]. Relative efficiency losses of up to 10% are measured in the bottom part of both upgraded metallurgical grade (UMG) mc-Si [26] and B-doped high performance (HP) mc-Si bricks [28]. Both materials show only partial recovery at 200 °C [26,28], and the HPmc-Si cells exhibit the strongest degradation near the grain boundaries (a.k.a. Sponge-LID) [28]. UMG feedstock does not appear to increase LID in QuMo-Si [176].

Passivated Emitter Rear Cells (PERC) are particularly sensitive to strong but slow LID, known as LeTID or LID2 [25,29,30]. As both the degradation rate [25] and the defect density [29] increase with increasing temperature, degradation results are mostly reported at $50-80$ °C. LeTID of over 10% is also measured in PERC Cz-Si cells with partial recovery at 200 °C and almost complete regeneration at 70 °C [29], suggesting that the cell structure and specifically the back-surface passivation layer causes the degradation. Even though aluminum oxide (Al_2O_3) passivation has previously been observed to improve during illumination [177,178], no significant LeTID difference is detected between PERC mc-Si with an Al_2O_3/SiN_x stack or simple SiN_x backside passivation [30]. LeTID is also observed in Ga-doped Al-BSF mc-Si cells [25], which cannot be explained by either passivation degradation or BO-LID. In AlO_x-passivated PERC mc-Si, Krauss et al. [170] correlate a low LeTID-related lifetime with high dislocation densities. In QuMo-Si, a high dislocation density appears to increase the degradation activation energy from 0.44 ± 0.01 to 0.57 ± 0.02 eV [179], without causing severe LeTID in QuMo PERC cells [25].

6. Conclusions

Although several types of light-induced degradation have been observed in crystalline silicon during the past 40 years, the specific recombination-active defects remain unknown. Clean Cz-Si suffers from BO-LID, which can be identified by two-step degradation and full recovery at 200 °C. BO-LID can be mitigated by illumination at 65–230 °C, provided that the surface passivation layer contains enough hydrogen.

If the Cz-Si wafer contains interstitial copper, Cu-LID appears as three-step degradation with fast, slow, and very slow decays. In contrast to BO-LID, Cu-LID shows either no or only partial recovery at 200 °C. Although Cu-LID cannot be diagnosed by total copper concentration measurements, Cu-LID may be confirmed by applying copper removal techniques, such as enhanced segregation gettering or copper out-diffusion.

Finally, modern multicrystalline silicon solar cells show mostly single exponential degradation. Many mc-Si wafers exhibit less detrimental LID than similarly doped Cz-Si, but particularly strong LID (also known as LeTID or LID2) has recently been observed in some mc-Si PERC and Al-BSF cells. Back-surface passivation may affect LeTID in B-doped mc-Si PERC, but Ga-doped mc-Si Al-BSF cells appear to suffer from bulk degradation.

In summary, light-induced degradation is a multifaceted problem in silicon solar cells, which will continue generating controversy within the industry and academia, until the responsible defects are identified. A plethora of additional degradation properties, defect models, and mitigation techniques are to be expected before all types of LID can be minimized in crystalline silicon solar cells.

Acknowledgments

J.L. acknowledges the financial support of the Characterization and Modeling of Materials (CMM) Group at Karlstad University and Walter Ahlström Foundation. H.S. acknowledges the support of the European Research Council under the European Union's Seventh Framework Programme (FP7/2007-2013)/ERC Grant Agreement no. 307315.

References

[1] H. Hashigami, Y. Itakura, T. Saitoh, Effect of illumination conditions on Czochralski-grown silicon solar cell degradation, J. Appl. Phys. 93 (2003) 4240–4245.
[2] K. Bothe, R. Hezel, J. Schmidt, Recombination-enhanced formation of the metastable boron-oxygen complex in crystalline silicon, Appl. Phys. Lett. 83 (2003) 1125–1127.
[3] R.L. Crabb, Photon induced degradation of electron irradiated silicon solar cells, in: Proceedings of the 9th IEEE Photovoltaic Specialists Conference, IEEE, Silver Springs, MD, USA, 1972, pp. 243–249.
[4] J. Schmidt, A.A. Aberle, R. Hezel, Investigation of carrier lifetime instabilities in Cz-grown silicon, in: Proceedings of the 26th IEEE Photovoltaic Specialist Conference, Anaheim, CA, USA, 1997, pp. 13–18.
[5] K. Graff, H. Pieper, Carrier lifetime measurements on electron-irradiated silicon crystals, Phys. Status Solidi A 30 (1975) 593–599.
[6] H. Fischer, W. Pschunder, Investigation of photon and thermal induced changes in silicon solar cells, in: Proceedings of the 10th IEEE Photovoltaic Specialist Conference, Palo Alto, CA, USA, 1973, pp. 404–411.
[7] D.J. Curtin, R.L. Statler, Review of radiation damage to silicon solar cells, IEEE Trans. Aerosp. Electron. Syst. AES-11 (1975) 499–513.
[8] S.W. Glunz, S. Rein, W. Warta, J. Knobloch, W. Wettling, Degradation of carrier lifetime in Cz silicon solar cells, Sol. Energy Mater. Sol. Cells 65 (2001) 219–229.
[9] K. Bothe, J. Schmidt, R. Hezel, Comprehensive analysis of the impact of boron and oxygen on the metastable defect in Cz silicon, in: Proceedings of the 3rd World Conference on Photovoltaic Energy Conversion, Osaka, Japan, 2003, pp. 1077–1080.
[10] J. Schmidt, K. Bothe, R. Hezel, Structure and transformation of the metastable centre in Cz-silicon solar cells, in: Proceedings of the 3rd World Conference on Photovoltaic Energy Conversion, Osaka, Japan, 2003, pp. 2887–2892.
[11] H. Hashigami, M. Dhamrin, T. Saitoh, Fast initial light-induced degradation of Czochralski silicon solar cells, in: Proceedings of the 3rd World Conference on Photovoltaic Energy Conversion, Osaka, Japan, 2003, pp. 1116–1119.
[12] C. Möller, K. Lauer, Light-induced degradation in indium-doped silicon, Phys. Status Solidi RRL 7 (2013) 461–464.
[13] C. Möller, K. Lauer, ASi-Sii-defect model of light-induced degradation in silicon, Energy Procedia 55 (2014) 559–563.
[14] S.W. Glunz, S. Rein, J. Knobloch, W. Wettling, T. Abe, Comparison of boron- and gallium-doped p-type Czochralski silicon for photovoltaic application, Prog. Photovolt. 7 (1999) 463–469.
[15] W.B. Henley, D.A. Ramappa, L. Jastrezbski, Detection of copper contamination in silicon by surface photovoltage diffusion length measurements, Appl. Phys. Lett. 74 (1999) 278–280.
[16] H. Savin, M. Yli-Koski, A. Haarahiltunen, Role of copper in light induced minority-carrier lifetime degradation of silicon, Appl. Phys. Lett. 95 (2009) 152111.
[17] J. Lindroos, M. Yli-Koski, A. Haarahiltunen, M.C. Schubert, H. Savin, Light-induced degradation in copper-contaminated gallium-doped silicon, Phys. Status Solidi Rapid Res. Lett. 7 (2013) 262–264.
[18] M.B. Shabani, T. Yamashita, E. Morita, Metallic impurities in mono and multicrystalline silicon and their gettering by phosphorus diffusion, ECS Trans. 16 (2008) 179–193.
[19] D.P. Fenning, A.S. Zuschlag, M.I. Bertoni, B. Lai, G. Hahn, T. Buonassisi, Improved iron gettering of contaminated multicrystalline silicon by high-temperature phosphorus diffusion, J. Appl. Phys. 113 (2013) 214504.

[20] D. Macdonald, A. Cuevas, A. Kinomura, Y. Nakano, Phosphorus gettering in multicrystalline silicon studied by neutron activation analysis, in: Proceedings of the 29th IEEE Photovoltaic Specialist Conference, IEEE, New Orleans, LA, USA, 2002, pp. 285–288.
[21] A. Bentzen, A. Holt, R. Kopecek, G. Stokkan, J.S. Christensen, B.G. Svensson, Gettering of transition metal impurities during phosphorus emitter diffusion in multicrystalline silicon solar cell processing, J. Appl. Phys. 99 (2006) 093509.
[22] T. Buonassisi, M.A. Marcus, A.A. Istratov, M. Heuer, T.F. Ciszek, B. Lai, Z. Cai, E. R. Weber, Analysis of copper-rich precipitates in silicon: chemical state, gettering, and impact on multicrystalline silicon solar cell material, J. Appl. Phys. 97 (2005) 063503.
[23] T. Turmagambetov, S. Dubois, J.-P. Garandet, B. Martel, N. Enjalbert, J. Veirman, E. Pihan, Influence of copper contamination on the illuminated forward and dark reverse current-voltage characteristics of multicrystalline p-type silicon solar cells, Phys. Status Solidi C 11 (2014) 1697–1702.
[24] D. Macdonald, A. Cuevas, A. Kinomura, Y. Nakano, L.J. Geerligs, Transition-metal profiles in a multicrystalline silicon ingot, J. Appl. Phys. 97 (2005) 033523.
[25] K. Ramspeck, S. Zimmermann, H. Nagel, A. Metz, Y. Gassenbauer, B. Birkmann, A. Seidl, Light induced degradation of rear passivated mc-Si solar cells, in: Proceedings of the 27th European Photovoltaic Solar Energy Conference and Exhibition, Frankfurt, Germany, 2012, pp. 861–865.
[26] S. Pingel, D. Koshnicharov, O. Frank, T. Geipel, Y. Zemen, B. Striner, J. Berghold, Initial degradation of industrial silicon solar cells in solar panels, in: Proceedings of the 25th European Photovoltaic Solar Energy Conference and Exhibition, Valencia, Spain, 2010, pp. 4027–4032.
[27] F. Fertig, K. Krauß, I. Geisemeyer, J. Broisch, H. Höffler, J.O. Odden, A.-K. Soiland, S. Rein, Fully solderable large-area screen-printed Al-BSF p-type mc-Si solar cells from 100% solar grade feedstock yielding $\eta > 17\%$: Challenges and potential on cell and module level, in: Proceedings of the 27th European Photovoltaic Solar Energy Conference and Exhibition, Frankfurt, Germany, 2012, pp. 1031–1038.
[28] C. Fahrland, Y. Ludwig, F. Kersten, K. Petter, Sponge LID - a new degradation mechanism? in: Proceedings of the 40th IEEE Photovoltaic Specialist Conference, Denver, CO, USA, 2014, pp. 0135–0139.
[29] F. Fertig, K. Krauß, S. Rein, Light-induced degradation of PECVD aluminium oxide passivated silicon solar cells, Phys. Status Solidi Rapid Res. Lett. 9 (2015) 41–46.
[30] F. Kersten, P. Engelhart, H.-C. Ploigt, A. Stekolnikov, T. Lindner, F. Stenzel, M. Bartzsch, A. Szpeth, K. Peter, J. Heitmann, J.W. Müller, Degradation of multicrystalline silicon solar cells and modules after illumination at elevated temperature, Sol. Energy Mater. Sol. Cells 142 (2015) 83–86.
[31] J. Lindroos, Copper-related light-induced degradation in crystalline silicon (Ph.D. thesis), Aalto University, Finland, 37/2015, 2015.
[32] T.U. Nærland, Characterization of light induced degradation in crystalline silicon (Ph.D. thesis), Norwegian University of Science and Technology, Trondheim, 2013 (2013) 303.
[33] J. Knobloch, S.W. Glunz, D. Biro, W. Warta, E. Schaffer, W. Wettling, Solar cells with efficiencies above 21% processed from Czochralski grown silicon, in: Proceedings of the 25th IEEE Photovoltaic Specialist Conference, Washington DC, USA, 1996, pp. 405–408.
[34] T.U. Nærland, H. Angelskår, M. Kirkengen, R. Søndenå, E.S. Marstein, The role of excess carriers in light-induced degradation examined by photoluminescence imaging, J. Appl. Phys. 112 (2012) 033703.
[35] T.U. Nærland, H. Angelskår, E.S. Marstein, Direct monitoring of minority carrier density during light induced degradation in Czochralski silicon by photoluminescence imaging, J. Appl. Phys. 113 (2013) 193707.
[36] K. Bothe, J. Schmidt, Electrically activated boron-oxygen-related recombination centers in crystalline silicon, J. Appl. Phys. 99 (2006) 013701.
[37] D.W. Palmer, K. Bothe, J. Schmidt, Kinetics of the electronically stimulated formation of a boron-oxygen complex in crystalline silicon, Phys. Rev. B 76 (2007) 035210.
[38] D.K. Schroder, Carrier lifetimes in silicon, IEEE Trans. Electron 44 (1997) 160–170.
[39] V.V. Voronkov, R. Falster, Light-induced boron-oxygen recombination centers in silicon: Understanding their formation and elimination, Solid State Phenom. 205–206 (2014) 3–14.
[40] V.V. Voronkov, R. Falster, Latent complexes of interstitial boron and oxygen dimers as a reason for degradation of silicon-based solar cells, J. Appl. Phys. 107 (2010) 053509.
[41] P. Hamer, B. Hallam, M. Abbott, S. Wenham, Accelerated formation of the boron-oxygen complex in p-type Czochralski silicon, Phys. Status Solidi Rapid Res. Lett. 9 (2015) 297–300.
[42] D. Macdonald, F. Rougieux, A. Cuevas, B. Lim, J. Schmidt, M. Di Sabatino, L. J. Geerligs, Light-induced boron-oxygen defect generation in compensated p-type Czochralski silicon, J. Appl. Phys. 105 (2009) 093704.
[43] S. Rein, S.W. Glunz, Electronic properties of the metastable defect in boron-doped Czochralski silicon: unambiguous determination by advanced lifetime spectroscopy, Appl. Phys. Lett. 82 (2003) 1054–1056.
[44] J. Schmidt, A. Cuevas, Electronic properties of light-induced recombination centers in boron-doped Czochralski silicon, J. Appl. Phys. 86 (1999) 3175–3180.
[45] T. Mchedlidze, J. Weber, Direct detection of carrier traps in Si solar cells after light-induced degradation, Phys. Status Solidi Rapid Res. Lett. 9 (2015) 108–110.
[46] T. Niewelt, J. Schön, J. Broisch, W. Warta, M.C. Schubert, Electrical characterization of the slow boron oxygen defect component in Czochralski silicon, Phys. Status Solidi Rapid Res. Lett. (2015) 1–5, http://dx.doi.org/10.1002/pssr.201510357.
[47] V.V. Voronkov, R. Falster, K. Bothe, B. Lim, J. Schmidt, Lifetime-degrading boron-oxygen centres in p-type and n-type compensated silicon, J. Appl. Phys. 110 (2011) 063515.
[48] B. Lim, V.V. Voronkov, R. Falster, K. Bothe, J. Schmidt, Lifetime recovery in p-type Czochralski silicon due to the reconfiguration of boron-oxygen complexes via a hole-emitting process, Appl. Phys. Lett. 98 (2011) 162104.
[49] M. Forster, E. Fourmond, F.E. Rougieux, A. Cuevas, R. Gotoh, K. Fujiwara, S. Uda, M. Lemiti, Boron-oxygen defect in Czochralski-silicon co-doped with gallium and boron, Appl. Phys. Lett. 100 (2012) 042110.
[50] M. Forster, P. Wagner, J. Degoulange, R. Einhaus, G. Galbiati, F. Rougieux, A. Cuevas, E. Fourmond, Impact of compensation on the boron and oxygen-related degradation of upgraded metallurgical-grade silicon solar cells, Sol. Energy Mater. Sol. Cells 120 (2014) 390–395.
[51] R. Kopecek, J. Arumughan, K. Peter, E.A. Good, J. Libal, M. Acciarri, S. Binetti, Crystalline Si solar cells from compensated material: Behaviour of light induced degradation, in: Proceedings of the 23rd European Photovoltaic Solar Energy Conference and Exhibition, Valencia, Spain, 2008, pp. 1855–1858.
[52] B. Lim, F. Rougieux, D. Macdonald, K. Bothe, J. Schmidt, Generation and annihilation of boron-oxygen-related recombination centers in compensated p- and n-type silicon, J. Appl. Phys. 108 (2010) 103722.
[53] K. Bothe, J. Schmidt, R. Hezel, Effective reduction of the metastable defect concentration in boron-doped Czochralski silicon for solar cells, in: Proceedings of the 29th IEEE Photovoltaic Specialists Conference, IEEE, New Orleans, LA, USA, 2002, pp. 194–197.
[54] V.V. Voronkov, R. Falster, K. Bothe, B. Lim, Light-induced lifetime degradation in boron-doped Czochralski silicon: Are oxygen dimers involved?, Energy Procedia 38 (2013) 636–641.
[55] J.R. Davis, A. Rohatgi, R.H. Hopkins, P.D. Blais, P. Rai-Choudhury, J. R. McCormick, H.C. Mollenkopf, Impurities in silicon solar cells, IEEE Trans. Electron Devices 4 (1980) 677–687.
[56] J. Schmidt, Temperature- and injection-dependent lifetime spectroscopy for the characterization of defect centers in semiconductors, Appl. Phys. Lett. 82 (2003) 2178–2180.
[57] P. Rosenits, T. Roth, S.W. Glunz, S. Beljakowa, Determining the defect parameters of the deep aluminum-related defect center in silicon, Appl. Phys. Lett. 91 (2007) 122109.
[58] L.J. Caballero, C. del Cañizo, P. Sánchez-Friera, A. Luque, Influence of P gettering thermal step on light-induced degradation in Cz Si, Sol. Energy Mater. Sol. Cells 88 (2005) 247–256.
[59] J. Fodor, R. Opjorden, Advanced silicon materials for space solar cells, in: Proceedings of the 14th IEEE Photovoltaic Specialist Conference, IEEE, San Diego, CA, USA, 1980, pp. 882–886.
[60] F.A. Trumbore, Solid solubilities of impurity elements in germanium and silicon, Bell Syst. Tech. J. 39 (1960) 205–233.
[61] S.W. Glunz, S. Rein, W. Warta, J. Knobloch, W. Wettling, On the degradation of Cz-silicon solar cells, in: Proceedings of the 2nd World Conference and Exhibition on Photovoltaic Solar Energy Conversion, Vienna, Austria, 1998, pp. 1343–1346.
[62] A. Herguth, G. Schubert, M. Kaes, G. Hahn, A new approach to prevent the negative impact of the metastable defect in boron doped Cz silicon solar cells, in: Proceedings of the 4th World Conference on Photovoltaic Energy Conversion, IEEE, Waikoloa, HI, USA, 2006, pp. 940–943.
[63] A. Herguth, G. Schubert, M. Kaes, G. Hahn, Investigations on the long time behavior of the metastable boron-oxygen complex in crystalline silicon, Prog. Photovolt. 16 (2008) 135–140.
[64] B. Lim, K. Bothe, J. Schmidt, Deactivation of the boron-oxygen recombination center in silicon by illumination at elevated temperature, Phys. Status Solidi RRL 2 (2008) 93–95.
[65] S. Wilking, A. Herguth, G. Hahn, Influence of hydrogen on the regeneration of boron-oxygen related defects in crystalline silicon, J. Appl. Phys. 113 (2013) 194503.
[66] B. Lim, A. Liu, D. Macdonald, K. Bothe, J. Schmidt, Impact of dopant compensation on the deactivation of boron-oxygen recombination centers in crystalline silicon, Appl. Phys. Lett. 95 (2009) 232109.
[67] B. Lim, K. Bothe, J. Schmidt, Impact of oxygen on the permanent deactivation of boron-oxygen-related recombination centers in crystalline silicon, J. Appl. Phys. 107 (2010) 123707.
[68] K. A. Münzer, Hydrogenated silicon nitride for regeneration of light induced degradation, in: Proceedings of the 24th European Photovoltaic Solar Energy Conference, Hamburg, Germany, 2009, pp. 1558–1561.
[69] G. Krugel, W. Wolke, J. Geilker, S. Rein, R. Preu, Impact of hydrogen concentration on the regeneration of light induced degradation, Energy Procedia 8 (2011) 47–51.
[70] S. Wilking, C. Beckh, S. Ebert, A. Herguth, G. Hahn, Influence of bound hydrogen states on BO-regeneration kinetics and consequences for high-speed regeneration processes, Sol. Energy Mater. Sol. Cells 131 (2014) 2–8.
[71] A. Herguth, G. Hahn, Kinetics of the boron-oxygen related defect in theory and experiment, J. Appl. Phys. 108 (2010) 114509.
[72] S. Wilking, P. Engelhart, S. Ebert, C. Beckh, A. Herguth, G. Hahn, High speed regeneration of BO-defects: Improving long-term solar cell performance within seconds, in: Proceedings of the 29th European Photovoltaic Solar

Energy Conference and Exhibition, Amsterdam, Netherlands, 2014, pp. 366–372.
[73] G. Hahn, S. Wilking, A. Herguth, BO-related defects: Overcoming bulk lifetime degradation in crystalline Si by regeneration, Solid State Phenom. 242 (2015) 80–89.
[74] I. Tarasov, S. Ostapenko, S.S. Koveshnikov, Light induced defect reactions in boron-doped silicon: Cu versus Fe, in: Proceedings of the 8th Workshop on Crystalline Silicon Solar Cell Materials and Process, Copper Mountain, CO, USA, 1998, pp. 207–210.
[75] M.B. Shabani, T. Yoshimi, H. Abe, Low-temperature out-diffusion of Cu from silicon wafers, J. Electrochem. Soc. 143 (1996) 2025–2029.
[76] D.A. Ramappa, Surface photovoltage analysis of phase transformation of copper in p-type silicon, Appl. Phys. Lett. 76 (2000) 3756–3758.
[77] J. Lindroos, Y. Boulfrad, M. Yli-Koski, H. Savin, Preventing light-induced degradation in multicrystalline silicon, J. Appl. Phys. 115 (2014) 154902.
[78] Y. Boulfrad, J. Lindroos, M. Wagner, F. Wolny, M. Yli-Koski, H. Savin, Experimental evidence on removing copper and light-induced degradation from silicon by negative charge, Appl. Phys. Lett. 105 (2014) 182108.
[79] A. Belayachi, T. Heiser, J.P. Schunck, A. Kempf, Influence of light on interstitial copper in p-type silicon, Appl. Phys. A 80 (2005) 201–204.
[80] H. Väinölä, E. Saarnilehto, M. Yli-Koski, A. Haarahiltunen, J. Sinkkonen, G. Berenyi, T. Pavelka, Quantitative copper measurement in oxidized p-type silicon wafers using microwave photoconductivity decay, Appl. Phys. Lett. 87 (2005) 032109.
[81] J. Lindroos, H. Savin, Formation kinetics of copper-related light-induced degradation in crystalline silicon, J. Appl. Phys. 116 (2014) 234901.
[82] H. Väinölä, M. Yli-Koski, A. Haarahiltunen, J. Sinkkonen, Sensitive copper detection in p-type Cz silicon using μ-PCD, J. Electrochem. Soc. 150 (2003) G790–G794.
[83] M. Yli-Koski, Optical activation of copper in silicon studied by carrier lifetime measurements (Ph.D. thesis), Helsinki University of Technology, Finland, 2004/31, 2004.
[84] Y. Boulfrad, J. Lindroos, A. Inglese, M. Yli-Koski, H. Savin, Reduction of light-induced degradation of boron-doped solar-grade Czochralski silicon by corona charging, Energy Procedia 38 (2013) 531–535.
[85] J. Lindroos, M. Yli-Koski, A. Haarahiltunen, H. Savin, Room-temperature method for minimizing light-induced degradation in crystalline silicon, Appl. Phys. Lett. 101 (2012) 232108.
[86] M. Yli-Koski, M. Palokangas, A. Haarahiltunen, H. Väinölä, J. Storgårds, H. Holmberg, J. Sinkkonen, Detection of low-level copper contamination in p-type silicon by means of microwave photoconductive decay measurements, J. Phys. Condens. Matter 14 (2002) 13119–13125.
[87] S.K. Estreicher, Rich chemistry of copper in crystalline silicon, Phys. Rev. B 60 (1999) 5375–5382.
[88] E.R. Weber, Transition metals in silicon, Appl. Phys. A 30 (1983) 1–22.
[89] A.A. Istratov, C. Flink, H. Heislmair, E.R. Weber, T. Heiser, Intrinsic diffusion coefficient of interstitial copper in silicon, Phys. Rev. Lett. 81 (1998) 1243–1246.
[90] S.K. Estreicher, D.J. Backlund, C. Carbogno, M. Scheffler, Activation energies for diffusion of defects in silicon: The role of the exchange-correlation functional, Angew. Chem., International Edition 50 (2011) 10221–10225.
[91] G. Mills, H. Jonsson, Quantum and thermal effects in H2 dissociative adsorption: Evaluation of free energy barriers in multidimensional quantum systems, Phys. Rev. Lett. 72 (1994) 1124–1128.
[92] H. Jonsson, G. Mills, K.W. Jacobsen, Nudged elastic band method for finding minimum energy paths of transitions, in: B.J. Berne, G. Ciccotti, D.F. Coker (Eds.), Classical and Quantum Dynamics in Condensed Phase Simulations, World Scientific, Singapore, 1998, pp. 385–404.
[93] G. Henkelman, B.P. Uberuaga, H. Jonsson, A climbing image nudged elastic band method for finding saddle points and minimum energy paths, J. Chem. Phys. 113 (2000) 9901–9904.
[94] G. Henkelman, H. Jonsson, Improved tangent estimate in the nudged elastic band method for finding minimum energy paths and saddle points, J. Chem. Phys. 113 (2000) 9978–9985.
[95] P. Wagner, H. Hage, H. Prigge, T. Prescha, J. Weber, Properties of copper-induced complexes in silicon, in: H.R. Huff, K.G. Barraclough, J.-I. Chikawa (Eds.), Semiconductor Silicon-1990, The Electrochemical Society, Pennington, NJ, 1990, pp. 675–686.
[96] A.A. Istratov, H. Heislmair, C. Flink, T. Heiser, E.R. Weber, Interstitial copper-related center in n-type silicon, Appl. Phys. Lett. 71 (1997) 2349–2351.
[97] C. Flink, H. Feick, S.A. McHugo, W. Seifert, H. Hieslmair, T. Heiser, A. A. Istratov, E.R. Weber, Out-diffusion and precipitation of copper in silicon: An electrostatic model, Phys. Rev. Lett. 85 (2000) 4900–4903.
[98] M. Seibt, M. Greiss, A.A. Istratov, H. Hedemann, A. Sattler, W. Schröter, Formation and properties of copper silicide precipitates in silicon, Phys. Status Solidi A 166 (1998) 171–182.
[99] M. Seibt, H. Hedemann, A.A. Istratov, F. Riedel, A. Sattler, W. Schröter, Structural and electrical properties of metal silicide precipitates in silicon, Phys. Status Solidi A 171 (1999) 301–310.
[100] M. Seibt, Homogeneous and heterogeneous precipitation of copper in silicon, in: H.R. Huff, K.G. Barraclough, J.-I. Chikawa (Eds.), Semiconductor Silicon-1990, The Electrochemical Society, Pennington, NJ, 1990, pp. 663–674.
[101] A.A. Istratov, H. Hedemann, M. Seibt, O.F. Vyvenko, W. Schröter, T. Heiser, C. Flink, H. Hieslmair, E.R. Weber, Electrical and recombination properties of copper-silicide precipitates in silicon, J. Electrochem. Soc. 145 (1998) 3889–3898.
[102] H. Prigge, P. Gerlach, P.O. Hahn, A. Schnegg, H. Jacob, Acceptor compensation in silicon induced by chemomechanical polishing, J. Electrochem. Soc. 138 (1991) 1385–1389.
[103] M. Miyazaki, Recombination Lifetime Measurements in Silicon, ASTM, West Conshohockens, PA (1998), p. 294–304.
[104] J.-G. Lee, S.R. Morrison, Copper passivation of dislocations in silicon, J. Appl. Phys. 64 (1988) 6679–6683.
[105] S. Naito, T. Nakashizu, Electric degradation and defect formation of silicon due to Cu, Fe, and Ni contamination, in: Defect Engineering in Semiconductor Growth, Processing and Device Technology, vol. 262, Materials Research Society, 1992, pp. 641–652.
[106] R. Sachdeva, A.A. Istratov, E.R. Weber, Recombination activity of copper in silicon, Appl. Phys. Lett. 79 (2001) 2937–2939.
[107] M. Yli-Koski, H. Väinölä, A. Haarahiltunen, J. Storgårds, E. Saarnilehto, J. Sinkkonen, Light activated copper defects in p-type silicon studied by PCD, Phys. Scr. T T114 (2004) 69–72.
[108] A. Inglese, J. Lindroos, H. Savin, Accelerated light-induced degradation for detecting copper contamination in p-type silicon, Appl. Phys. Lett. 105 (2015) 052101.
[109] M. Boehringer, J. Hauber, S. Passefort, K. Eason, In-line copper contamination monitoring using noncontact Q-SPV techniques, J. Electrochem. Soc. 152 (2005) G1–G6.
[110] M. Nakamura, S. Murakami, N.J. Kawa, S. Saito, K. Matsukawa, H. Arie, Compositional transformation between Cu centers by annealing in Cu-diffused silicon crystals studied with deep-level transient spectroscopy and photoluminescence, Jpn. J. Appl. Phys. 48 (2009) 082302.
[111] J. Weber, H. Bauch, R. Sauer, Optical properties of copper in silicon: Excitons bound to isoelectronic copper pairs, Phys. Rev. B 25 (1982) 7688–7699.
[112] P.N. Hai, T. Gregorkiewicz, C.A.J. Ammerlaan, D.T. Don, Copper-related defects in silicon: electron-paramagnetic-resonance identification, Phys. Rev. B 56 (1997) 4620–4625.
[113] M.L.W. Thewalt, M. Steger, A. Yang, N. Stavrias, M. Cardona, H. Riemann, N. V. Abrosimov, M.F. Churbanov, A.V. Gusev, A.D. Bulanov, I.D. Kovalev, A. K. Kaliteevskii, O.N. Godisov, P. Becker, H.-J. Pohl, J.W. Ager, E.E. Haller, Can highly enriched 28Si reveal new things about old defects? Phys. B 401 (2007) 587–592.
[114] M. Steger, A. Yang, N. Stavrias, M.L.W. Thewalt, H. Riemann, N.V. Abrosimov, M.F. Churbanov, A.V. Gusev, A.D. Bulanov, I.D. Kovalev, A.K. Kaliteevskii, O. N. Godisov, P. Becker, H.-J. Pohl, Reduction of the linewidths of deep luminescence centers in 28Si reveals fingerprints of the isotope constituents, Phys. Rev. Lett. 100 (2008) 177402.
[115] M. Nakamura, S. Murakami, H. Udono, Transformation reactions of copper centers in the space-charge region of a copper-diffused silicon crystal measured by deep-level transient spectroscopy, J. Appl. Phys. 112 (2012) 063530.
[116] M. Nakamura, S. Murakami, Deep-level transient spectroscopy and photoluminescence measurements of dissociation energy of the 1.014-eV copper center in copper-diffused silicon crystal, J. Appl. Phys. 111 (2012) 073512.
[117] K. Shirai, H. Yamaguchi, A. Yanase, H. Katayama-Yoshida, A new structure of Cu complex in Si and its photoluminescence, J. Phys.: Condens. Matter 21 (2009) 06429.
[118] S.K. Estreicher, A. Carvalho, The CuPL defect and the Cus1Cui3 complex, Phys. B 407 (2012) 2967–2969.
[119] J. Weber, L. Scheffler, V. Kolkovski, N. Yarykin, New results on the electrical activity of 3d-transition metal impurities in silicon, Solid State Phenom. 205–206 (2014) 245–254.
[120] S.K. Estreicher, D. West, P. Ordejon, Copper-defect and copper-impurity interactions in silicon, Solid State Phenom. 82–84 (2002) 341–347.
[121] D. West, S.K. Estreicher, Copper interactions with H, O, and the self-interstitial in silicon, Phys. Rev. B 68 (2003) 035210.
[122] V.P. Markevich, A.R. Peaker, I.F. Medvedeva, V.E. Gusakov, L.I. Murin, B. G. Svensson, Radiation-induced defect reactions in Cz-Si crystals contaminated with Cu, Solid State Phenom. 131–133 (2007) 363–368.
[123] L.C. Kimerling, J.L. Benton, J.J. Rubin, Transition metal impurities in silicon, in: R. Hasiguti (Ed.), Defects and radiation effects in semiconductors 1980, Inst. Phys. Conf. Ser., Institute of Physics, vol. 59, 1981, pp. 217–222.
[124] H. Lemke, Defect reactions in Cu-doped silicon-crystals, Phys. Status Solidi A 95 (1986) 665–677.
[125] H. Lemke, Substitutional transition metal defects in silicon grown-in by the float zone technique, in: M. Suezawa, H. Katayama-Yoshida (Eds.), Defects in Semiconductors, Mater. Sci. Forum, vol. 196–201, 1995, pp. 683–688.
[126] A. Mesli, T. Heiser, Defect reactions in copper-diffused and quenched p-type silicon, Phys. Rev. B 45 (1992) 11632–11641.
[127] M. Saritas, A.R. Peaker, Deep states associated with oxidation-induced stacking-faults in RTA p-type silicon before and after copper diffusion, Solid-State Electron. 38 (1995) 1025–1034.
[128] K. Graff, Metal Impurities in Silicon-Device Fabrication, 2nd ed., Springer, Berlin, Heidelberg, 2000.
[129] H. Lemke, Properties of copper donor levels in silicon, Phys. Status Solidi A 1 (1970) 283–286.
[130] M.M. Akhmedova, L.S. Berman, L.S. Kostina, A.A. Lebedev, Investigation of parameters of copper levels in silicon by capacitance methods, Sov. Phys. Semicond. USSR 10 (1976) 1400–1401.
[131] S.J. Pearton, A.J. Tavendale, Electrical properties of deep copper- and nickel-related centers in silicon, J. Appl. Phys. 54 (1983) 1375–1379.
[132] S.D. Brotherton, J.R. Ayres, A. Gill, H.W. Van Kesteren, F.J.A.M. Greidanus, Deep levels of copper in silicon, J. Appl. Phys. 62 (1987) 1826–1832.

[133] K.-M. Chen, G.-G. Qin, Cu-related deep levels in Si and the interaction between Cu and irradiation defects, in: H. von Bardeleben (Ed.), Defects in Semiconductors, Mater. Sci. Forum, vol. 10–12, 1986, pp. 1093–1098.
[134] S. Knack, J. Weber, H. Lemke, H. Riemann, Copper-hydrogen complexes in silicon, Phys. Rev. B 65 (2002) 165203.
[135] A. Mesli, T. Heiser, E. Mulheim, Copper diffusivity in silicon: A re-examination, Mater. Sci. Eng. B 25 (1994) 141–146.
[136] A.A. Istratov, E.R. Weber, Electrical properties and recombination activity of copper, nickel and cobalt in silicon, Appl. Phys. A 66 (1998) 123–136.
[137] J. Weber, H. Bauch, R. Sauer, Optical properties of copper in silicon: Excitons bound to isoelectronic copper pairs, Phys. Rev. B 25 (1982) 7688.
[138] M. Nakamura, Long-time stability of high-concentration copper complexes in silicon crystals, Appl. Phys. Lett. 79 (2001) 2904–2906.
[139] M. Nakamura, H. Iwasaki, Copper complexes in silicon, J. Appl. Phys. 86 (1999) 5372–5375.
[140] S. Koveshnikov, Y. Pan, H.C. Mollenkopf, Investigation of electronic states in copper doped p-type silicon, in: C.L. Claeys, P. Rai-Choudhury, P. Stallhofer, J. E. Maurits (Eds.), Proceedings of the Fourth International Symposium on High Purity Silicon, The Electrochemical Society, Pennington, NJ, 1996, pp. 473–480.
[141] M. Nakamura, S. Murakami, H. Udono, Energy level(s) of the dissociation product of the 1.014 eV photoluminescence copper center in n-type silicon determined by photoluminescence and deep-level transient spectroscopy, J. Appl. Phys. 114 (2013) 033508.
[142] W. Schröter, V. Kveder, M. Seibt, H. Ewe, H. Hedemann, F. Riedel, A. Sattler, Atomic structure and electronic states of nickel and copper silicides in silicon, Mater. Sci. Eng. B 72 (2000) 80–86.
[143] D. Macdonald, A. Cuevas, S. Rein, P. Lichtner, S.W. Glunz, Temperature- and injection-dependent lifetime spectroscopy of copper-related defects in silicon, in: Proceedings of the 3rd World Conference on Photovoltaic Energy Conversion, Osaka, Japan, 2003, pp. 87–90.
[144] J.K. Solberg, Crystal-structure of η-Cu3Si precipitates in silicon, Acta Crystallogr. Sect. A 34 (1978) 684–698.
[145] H. Gottschalk, Precipitation of copper silicide on glide dislocations in silicon at low temperature, Phys. Status Solidi A 137 (1993) 447–461.
[146] M. Seibt, W. Schröter, Formation and properties of metastable silicide precipitates in silicon, Solid State Phenom. 19 (1991) 283–294.
[147] M. Seibt, K. Graff, Characterization of haze-forming precipitates in silicon, J. Appl. Phys. 63 (1988) 4444–4450.
[148] M. Seibt, R. Khalil, V. Kveder, W. Schröter, Electronic states at dislocations and metal silicide precipitates in crystalline silicon and their role in solar cell materials, Appl. Phys. A 96 (2009) 235–253.
[149] A. Sattler, H. Hedemann, A.A. Istratov, M. Seibt, W. Schröter, The nature of the electronic states of Cu3Si-precipitates in silicon, Solid State Phenom. 63–4 (1998) 369–374.
[150] T. Buonassisi, M.D. Pickett, A.A. Istratov, E. Sauar, T.C. Lommasson, E.S. Marstein, T. Pernau, R.F. Clark, S. Narayanan, S.M. Heald, E.R. Weber, Interactions between metals and different grain boundary types and their impact on multicrystalline silicon device performance, in: Proceedings of the 4th World Conference on Photovoltaic Energy Conversion, IEEE, Waikoloa, HI, USA, 2006, pp. 944–947.
[151] S.A. McHugo, A. Mohammed, A.C. Thompson, B. Lai, Z. Cai, Copper precipitates in silicon: Precipitation, dissolution, and chemical state, J. Appl. Phys. 91 (2002) 6396–6405.
[152] D.K. Schroder, Semiconductor Material and Device Characterization, 3rd ed., Wiley, Hoboken, New Jersey, 2006.
[153] F.S. Ham, Theory of diffusion-limited precipitation, J. Phys. Chem. Solids 6 (1958) 335–351.
[154] S.A. McHugo, Release of metal impurities from structural defects in polycrystalline silicon, Appl. Phys. Lett. 71 (1997) 1984–1986.
[155] J. Arumughan, J. Theobald, M. Wilson, L. Hildebrand, R. Petres, A. Savtchouk, J. Lagowski, R. Kopecek, Lifetime degradation in dark observed in mono crystalline Cz-silicon, in: Proceedings of the 26th European Photovoltaic Energy Conference and Exhibition, Hamburg, Germany, 2011, pp. 1014–1016.
[156] D.A. Ramappa, W.B. Henley, Surface photovoltage analysis of copper in p-type silicon, Appl. Phys. Lett. 72 (1998) 2298–2300.
[157] A.A. Istratov, C. Flink, H. Heislmair, T. Heiser, E.R. Weber, Influence of interstitial copper on diffusion length and lifetime of minority carriers in p-type silicon, Appl. Phys. Lett. 71 (1997) 2121–2123.
[158] G. Kissinger, D. Kot, M. Klingsporn, M.A. Schubert, A. Sattler, T. Müller, Investigation of the copper gettering mechanism of oxide precipitates in silicon, ECS J. Solid State Sci. Technol. 4 (2015) N124–N129.
[159] K. Sueoka, Modeling of internal gettering of nickel and copper by oxide precipitates in Czochralski-Si wafers, J. Electrochem. Soc. 152 (2005) G731–G735.
[160] D. Kot, D. Kissinger, A. Sattler, W. von Ammon, Comparison of evaluation criteria for efficient gettering of Cu and Ni in silicon wafers, ECS Trans. 25 (2009) 67–78.
[161] T. Heiser, A. Belayachi, J.P. Schunck, Copper behavior in bulk silicon and associated characterization techniques, J. Electrochem. Soc. 150 (2003) G831–G837.
[162] Y. Kitagawara, H. Takeno, S. Tobe, Y. Hayam Izu, T. Koide, T. Takenaka, Systematic analyses of practical problems related to defects and metallic impurities in silicon, in: S. Ashok, J. Chevallier, W. Goetz, B.L. Sopori, K. Sumino (Eds.), Materials Research Society Symposium Proceedings, Mater. Res. Soc., vol. 510, 1998, pp. 3–14.
[163] L. Fabry, R. Hoelzl, A. Andrukhiv, K. Matsumoto, J. Qiu, S. Koveshnikov, M. Goldstein, A. Grabau, H. Horie, R. Takeda, Test methods for measuring bulk copper and nickel in heavily doped p-type silicon wafers, J. Electrochem. Soc. 153 (2006) G566–G571.
[164] D. Kot, D. Kissinger, A. Sattler, T. Müller, Development of a storage getter test for Cu contaminations in silicon wafers based on ToF-SIMS measurements, Acta Phys. Pol. A 125 (2014) 965–968.
[165] C. Modanese, G. Gaspar, L. Arnberg, M. Di Sabatino, On copper diffusion in silicon measured by glow discharge mass spectrometry, Anal. Bioanal. Chem. 406 (2014) 7455–7462.
[166] M.B. Shabani, S. Okuuchi, Y. Shimanuki, Kinetics of low-temperature out-diffusion of copper from silicon wafers, in: B.O. Kolbesen, C. Claeys, P. Stallhofer, F. Tardif, J. Benton, T. Shaffner, D. Schroder, S. Kishino, P. Rai-Choudhury (Eds.), Analytical and Diagnostic Techniques for Semiconductor Materials, Devices, and Processes, The Electrochemical Society, Pennington, NJ, vol. 99-16, 1999, pp. 510–525.
[167] K. Hozawa, S. Isomae, J. Yugami, Copper distribution near a SiO2/Si interface under low-temperature annealing, Jpn. J. Appl. Phys. 41 (2002) 5887–5893.
[168] R. Hoelzl, D. Huber, K.-J. Range, L. Fabry, J. Hage, R. Wahlich, Gettering of copper and nickel in p/p+ epitaxial wafers, J. Electrochem. Soc. 147 (2000) 2704–2710.
[169] R. Hoelzl, K.-J. Range, L. Fabry, Modeling of Cu gettering in p- and n-type silicon and in poly-silicon, Appl. Phys. A 75 (2002) 525–534.
[170] K. Krauß, F. Fertig, D. Menzel, S. Rein, Light-induced degradation of silicon solar cells with aluminium oxide passivated rear side, Energy Procedia 77 (2015) 599–606.
[171] J. Junge, A. Herguth, G. Hahn, D. Kreßner-Kiel, R. Zierer, Investigation of degradation in solar cells from different mc-Si materials, Energy Procedia 8 (2011) 52–57.
[172] H. Nagel, J. Schmidt, A.A. Aberle, R. Hezel, Exceptionally high bulk minority-carrier lifetimes in block-cast multicrystalline silicon, in: Proceedings of the 14th European Photovoltaic Solar Energy Conference, Barcelona, Spain, 1997, pp. 762–765.
[173] D. Macdonald, L.J. Geerligs, S. Riepe, Light-induced lifetime degradation in multicrystalline silicon, in: Proceedings of the 13th Workshop on Crystalline Silicon Solar Cell Materials and Processes, Vail, CO, USA, 2003, pp. 182–185.
[174] G. Coletti, C.L. Mulder, G. Galbiati, L.J. Geerligs, Reduced effect of B-O degradation on multicrystalline silicon wafers, in: Proceedings of the 21st European Photovoltaic Energy Conference and Exhibition, Dresden, Germany, 2006, pp. 1515–1518.
[175] S. Dubois, N. Enjalbert, J. Veirman, J.P. Garandet, F. Tanay, A. Jouini, J. Champliaud, Evidences on the carbon participation for the slowing down of the boron-oxygen defects activation kinetics in solar-grade silicon, in: Proceedings of the 6th International Workshop on Science and Technology of Crystalline Silicon Solar Cells, Aix-les-Bains, France, 2012.
[176] V. Parra, T. Carballo, D. Cancillo, B. Moralejo, O. Martinez, J. Jimenez, J. Bullon, J.M. Miguez, R. Ordas, Trends in crystalline silicon growth for low cost and efficient photovoltaic cells, in: Proceedings of the 2013 Spanish Conference on Electron Devices (CDE), Valladolid, Spain, 2013, pp. 305–308.
[177] G. Dingemans, P. Engelhart, R. Seguin, F. Einsele, B. Hoex, M.C.M. van den Sanden, W.M.M. Kessels, Stability of Al2O3 and Al2O3/a-SiNx:H stacks for surface passivation of crystalline silicon, J. Appl. Phys. 106 (2009) 114907.
[178] B. Liao, R. Stangl, T. Mueller, F. Lin, C.S. Bhatia, B. Hoex, The effect of light soaking on crystalline silicon surface passivation by atomic layer deposited Al2O3, J. Appl. Phys. 113 (2013) 024509.
[179] X. Gu, S. Yuan, K. Yu, X. Guo, D. Yang, Dislocation-induced variation of generation kinetics of boron-oxygen complexes in silicon, J. Cryst. Growth 359 (2012) 69–71.